International Journal of Heat and Mass Transfer 52 (2009) 100–111

Contents lists available at ScienceDirect

International Journal of Heat and Mass Transfer

journal homepage: www.elsevier.com/locate/ijhmt

A mathematical model for the spray freeze drying process: The drying of frozen particles in trays and in vials on trays

A.I. Liapis [a,*], R. Bruttini [b]

[a] Department of Chemical and Biological Engineering, Missouri University of Science and Technology, 400 W. 11th Street, Rolla, MO 65409-1230, USA
[b] Criofarma-Freeze Drying Equipment, Strada del Francese, 97/2L, 10156 Turin, Italy

ARTICLE INFO

Article history:
Received 27 February 2008
Received in revised form 14 June 2008
Available online 22 August 2008

Keywords:
Spray freeze drying
Drying of spray-frozen particles
Drying of frozen particles in packed beds
Mathematical model for spray freeze drying
Lyophilization of spray-frozen particles
Lyophilization of frozen particles in packed beds

ABSTRACT

A mathematical model is presented that can be used to study the heat and mass transfer mechanisms that determine the dynamic behavior of the primary and secondary drying stages of spray freeze drying (freeze drying of particle based materials) in trays and in vials on trays. Simulation results indicate that particle based materials require longer primary drying times than solution based materials (conventional freeze drying) due to (a) reductions in the heat and mass transfer capabilities of particle based materials, and (b) the development of a secondary porous dried layer near the surface of the lower heating plate during the primary drying stage of the spray freeze drying process. The results of spray freeze drying for the systems studied in this work indicate that the drying rate during the primary drying stage increases as (i) the product height decreases, (ii) the particle diameter increases, and (iii) the value of the packing porosity increases. The mathematical model presented in this work is considered to offer a necessary and essential capability that could be used for the design, optimization, and control of the spray freeze drying process as well as of a process involving the drying of frozen particles in packed beds.

1. Introduction

In the process of spray freeze drying [1–9] which involves the freeze drying of particle based products, a liquid stream that represents the solution of the solute (product of interest) and solvent (e.g., water) is atomized, frozen by contact with a freezing medium such as liquid nitrogen or a cold gas stream, and the frozen solvent is removed by sublimation during the primary drying stage by maintaining in the drying chamber pressure and temperature conditions below the triple point of the solvent (e.g., water). The sorbed (bound) solvent that remains in the matrix of the solute after the completion of the primary drying stage, is then further reduced by desorption during the secondary drying stage of the freeze drying process [10–14]. The low temperature and pressure conditions of spray freeze drying allow the stable dehydration of heat sensitive materials (e.g., pharmaproteins) with minimal quality degradation and also support the formation of highly porous structures inside the particles of the materials. The porous particles that are obtained from the spray freeze drying process have relatively small aerodynamic diameters (usually smaller than 5 μm) and large geometrical diameters (usually larger than 10 μm) and, thus, spray freeze drying represents a highly promising technology for the production of porous particles whose physical and aerosol characteristics are considered to be ideal for use in pulmonary drug delivery [1–4,6,8]. Furthermore, researchers have reported that spray freeze drying has the potential of being a process of choice in drug production not only for pulmonary drug delivery, but also in the processing of low water soluble drugs [5,9], the production of powders for epidermal immunization [6,7], and the preparation of particles for micro-encapsulation [1,2].

While the conventional freeze drying process employed in the pharmaceutical, fine chemicals, and biotechnology industries involves the freeze drying of solution based products where a liquid solution of a solute of interest is frozen on trays or in vials on trays followed by the primary drying stage where there is no water (solvent) vapor movement in the saturated frozen region (frozen solution) of the material and sublimation occurs in a very narrow region so that a moving sublimation interface is considered to exist and has been observed experimentally [10–19], spray freeze drying involves the packing of frozen particles in containers and, thus, a packed bed [20,21] of frozen particles is formed which has a porous structure that makes the frozen region of the material to be unsaturated during primary drying because the space of the frozen region formed by the packed frozen particles is partially filled with frozen liquid solution (frozen particles) and partially filled with gas (water vapor and inerts) which moves through the pores of the unsaturated [22–24] porous frozen region by convection and diffusion during primary drying, as per Fig. 1a and b. In effect, spray freeze drying involves the drying of unsaturated porous frozen

* Corresponding author. Tel.: +1 573 341 4414; fax: +1 314 965 9329.
E-mail address: ail@mst.edu (A.I. Liapis).

0017-9310/$ - see front matter © 2008 Elsevier Ltd. All rights reserved.
doi:10.1016/j.ijheatmasstransfer.2008.06.026

Nomenclature

c_p	heat capacity (kJ/kg)
c_{sw}	concentration of bound (sorbed) water (kg water/kg solid)
C_{01}	constant dependent only upon the structure of the porous medium and giving relative Darcy flow permeability (m^2)
C_1	constant dependent only upon the structure of the porous medium and giving relative Knudsen flow permeability (m)
C_2	constant dependent only upon the structure of the porous medium and giving the ratio of bulk diffusivity within the porous medium to the free gas bulk diffusivity (dimensionless)
d_{ice}	diameter of ice core in particle (m)
d_p	diameter of particle (m)
d_{pore}	mean pore diameter of porous layer formed from the packing of the particles (m)
$D_{w,in}$	free gas mutual diffusivity in a binary mixture of water vapor and inert gas (m^2/s)
$D^0_{w,in}$	$D_{w,in}P$ (N/s)
$H(t,r)$	geometric shape (as per Fig. 1b) of the moving interface, a function of time and radial distance (m)
k	thermal conductivity (W/K m)
k_1	bulk diffusivity constant, $k_1 = C_2 D^0_{w,in} K_w/(C_2 D^0_{w,in} + K_{mx}P)$ (m^2/s)
k_2, k_4	self-diffusivity constant, $k_2 = k_4 = (K_w K_{in}/(C_2 D^0_{w,in} + K_{mx}P)) + (C_{01}/\mu_{mx})$ (m^4/N s)
k_3	bulk diffusivity constant, $k_3 = C_2 D^0_{w,in} K_{in}/(C_2 D^0_{w,in} + K_{mx}P)$ (m^2/s)
k_{des}	rate constant in the desorption mechanism of bound water, Eq. (6) (s^{-1})
K_w	Knudsen diffusivity for water vapor, $K_w = C_1(R_g T/M_w)^{0.5}$ (m^2/s)
K_{in}	Knudsen diffusivity of inert gas, $K_{in} = C_1(R_g T/M_{in})^{0.5}$ (m^2/s)
K_{mx}	mean Knudsen diffusivity for binary gas mixture, $K_{mx} = y_w K_{in} + y_{in} K_w$ (m^2/s)
L	length (height) of material in tray or vial (m)
m_w	amount of free water in material (kg/m^2)
M	molecular weight (kg/kmol)
N	mass flux (kg/m^2 s)
p	partial pressure (Pa)
p_w^{sat}	saturated water vapor pressure (Pa)
P	total pressure (Pa)
P_{dcham}	pressure in drying chamber (Pa)
q	heat flux (W/m^2)
r	space coordinate of radial distance (m)
R	radius of vial (m)
R_g	ideal gas constant (J/K mol)
S	ice saturation, Eq. (7) (dimensionless)
S_{av}	volume-averaged ice saturation, Eq. (16) (dimensionless)
t	time (s)
T	temperature (K)
T_X	temperature at surface of moving interface (K)
V	velocity of moving interface (m/s)
x	space coordinate of distance along the length (height) of the material in the tray (m)
X	position of moving interface in the material in the tray (m)
y	mole fraction (dimensionless)
z	space coordinate of distance along the length of the vial (m)
Z	value of z at the moving interface in the vial (m)

Greek letters

ΔH_s	heat of sublimation of ice (J/kg)
ΔH_v	heat of vaporization of bound water (J/kg)
ε_p	particle porosity (dimensionless)
ε_{pb}	porosity of the bed formed by the packed particles (dimensionless)
ζ	parameter defined in Eq. (31) (dimensionless)
μ_{mx}	viscosity of vapor phase in the pores (kg/m s)
ρ	density (kg/m^3)
τ	tortuosity (dimensionless)

Superscripts

o	initial value

Subscripts

d	dried particle based material after primary drying
d,s	dried solution based material after primary drying
d,s,f	dried solution based material when frozen and sorbed water have been removed
e	effective
f	frozen particle based material
f,s	frozen solution based material
g	gas
I	region I, porous dried layer
II	region II, unsaturated porous frozen layer
in	inert gas
interf	moving interface
lp	lower heating plate
m	melting
mx	binary mixture of water vapor and inert gas
pd	primary drying stage
scor	scorch
t	total
up	upper heating plate
w	water vapor

media while conventional freeze drying involves the drying of saturated nonporous frozen solutions. But this is a very significant difference because in spray freeze drying the pore structure formed by the packed frozen particles provides transport channels (pores) for the movement (transport) of water (solvent) vapor in the unsaturated porous frozen region of the material being dried. Therefore, in spray freeze drying, in order to satisfy, as the water vapor moves through the pores of the frozen region, the local thermodynamic equilibrium and mass balance of water vapor, the ice (frozen solvent) will be sublimated or the water vapor will be condensed in the voids represented by the pores of the frozen region, and, thus, the saturation of frozen mass will decrease or increase. Wang and Shi [25,26] studied the sublimation–condensation phenomena taking place during microwave freeze drying of beef and called this region where changes in the saturation of frozen mass occur, a sublimation–condensation region . It is also important to indicate clearly here that in spray freeze drying each frozen particle during drying produces a porous structure of its own as the ice sublimates (as per Fig. 1c), and the pore structure of the dried particle depends on the initial formulation of the solution and the size distribution of the ice crystals that were formed [14,15] during the spraying of the solution into a freezing medium. Thus, the porous structure of the dried region of the material that is obtained during the primary drying stage of spray freeze drying is bidisperse

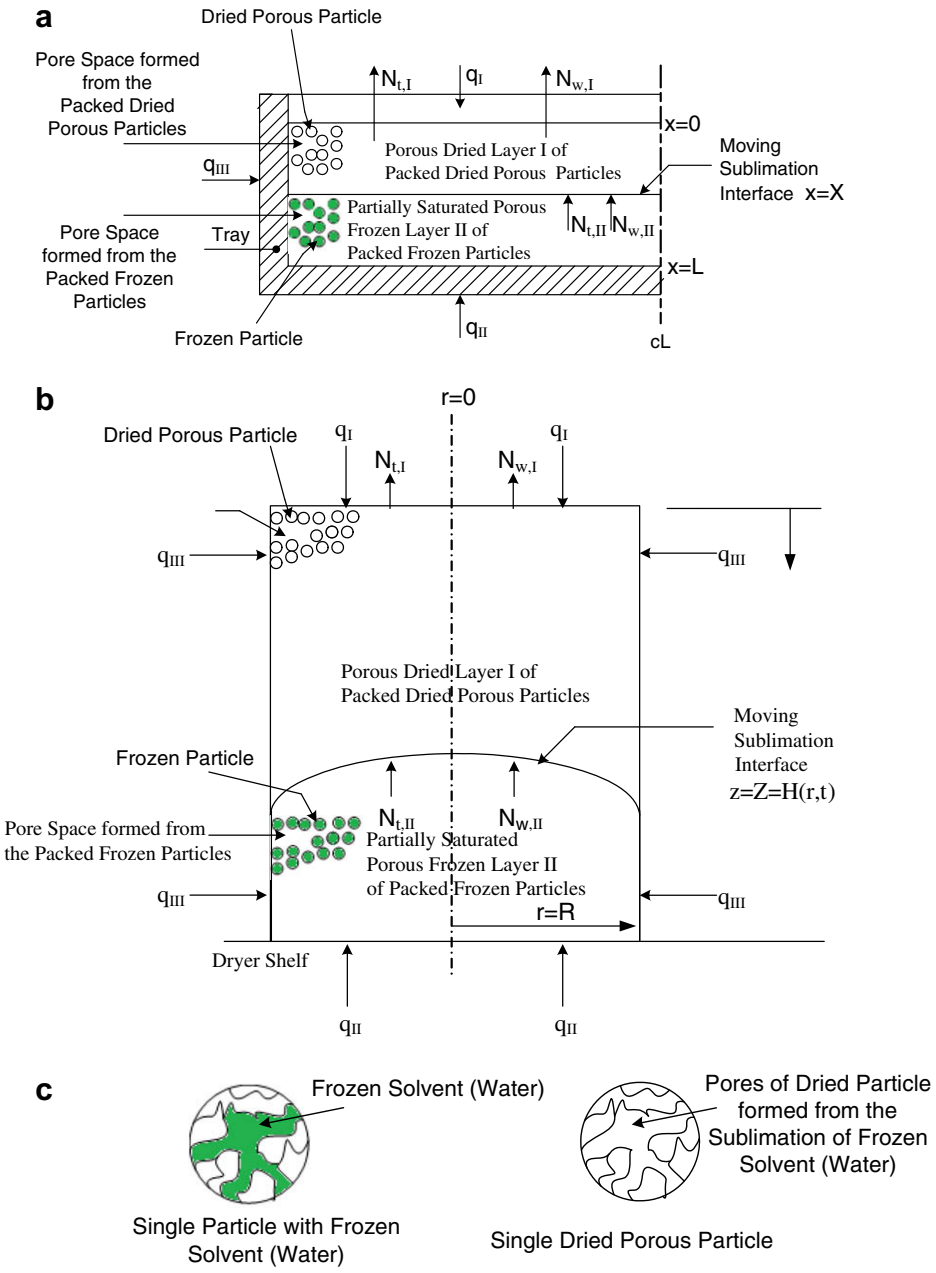

Fig. 1. (a) Diagram of a material being spray freeze dried in a tray (bulk spray freeze drying). (b) Diagram of a material being spray freeze dried in a vial on a tray. (c) Depictions of the frozen solvent (water) in a frozen particle and the pores resulting from the sublimation of frozen water during the primary drying stage to form a porous dried particle.

because the void space of the packed frozen particles is characterized by a pore size distribution and pore connectivity [27–29] that are different than the pore size distribution and pore connectivity that characterize the pore structure resulting from the drying of the individual frozen particles. In spray freeze drying the porous frozen region (partially saturated region) of the material being dried is separated from the porous dried region obtained during primary drying, as per Fig. 1, by a moving sublimation front, while in conventional freeze drying the moving sublimation front separates the nonporous frozen solution region (saturated region) from the porous dried region obtained during primary drying [10–14].

The increasing importance of spray freeze drying in the production of pulmonary inhalable drugs, in the processing of low water soluble drugs, in the production of powders for epidermal immunization, and in the preparation of particles for micro-encapsulation, requires knowledge about the heat and mass transfer mechanisms involved in the primary and secondary drying stages of the spray freeze drying process in order to construct control policies that reduce the long drying times and intensive use of energy to maintain the required operational conditions in the drying chamber, condenser, and vacuum pump system of the freeze dryer, so that increased productivity and lower operational costs could be realizable. Therefore, in order to establish both qualitative and quantitative control policies for the heat input, drying chamber pressure, and condenser temperature that can reduce substantially the drying times and exergy losses during the primary and secondary drying stages of spray freeze drying, as has been done for conventional freeze drying [10–12,14,15,17,18,30–36], a dynamic mathematical model that accounts properly for the heat and mass transfer mechanisms that are active in spray freeze drying during

the primary and secondary drying stages needs to be constructed and solved. In this work, a mathematical model that describes the dynamic behavior of spray freeze drying both in the porous frozen (partially saturated) region and in the dried region of the material being dried, is constructed and used to simulate the dynamic behavior of the spray freeze drying process.

2. System formulation

In Fig. 1a and b diagrams of a material on a tray and in a vial during spray freeze drying, respectively, are presented. The variables X and $Z = H(t,r)$ represent the position of the moving sublimation interface (front) between the partially saturated porous frozen layer II formed from the packed frozen particles and the porous dried layer I of the material on a tray and in a vial, respectively. In the pores of the porous frozen layer II, there is movement of gas (water vapor and inerts) while in the dried layer I there is also movement of gas and the water vapor is transported through the bidisperse porous structure of the dried layer I to the drying chamber where it is then removed and condensed in the water vapor condenser. During the primary drying stage the water vapor is mainly obtained from sublimation of ice (a negligible amount of water vapor is obtained from the desorption of bound water during primary drying [10,11,14]), while during the secondary drying stage the water vapor is obtained from the desorption of bound water. The end of the primary drying stage is taken to occur when (a) $X = L$ for the material being dried on trays [10,14], and (b) $Z = H(t,r) = L$ for $0 \leqslant r \leqslant R$ for the material being dried in vials located on trays [11,12,14]. The secondary drying stage begins at the end of the primary drying stage, and during the secondary drying stage there is no partially saturated porous frozen layer II and the only layer that exists is the bidisperse porous dried layer I. The variables q_{I}, q_{II}, and q_{III} in Fig. 1 denote the heat fluxes to the material supplied from the tray (heating plate) located above the material, the heating plate (tray) on which the material is located, and the drying chamber environment, respectively [10–12,14].

2.1. Mathematical model for the primary drying stage of spray freeze drying

For primary drying, the energy balance equation in the dried layer is as follows:

$$\rho_{\mathrm{Ie}} c_{\mathrm{pIe}} \frac{\partial T_{\mathrm{I}}}{\partial t} = \nabla \cdot (k_{\mathrm{Ie}} \nabla T_{\mathrm{I}}) - c_{\mathrm{pg}} (\nabla \cdot (N_{\mathrm{t,I}} T_{\mathrm{I}})) + \Delta H_{\mathrm{v}} \rho_{\mathrm{I}} \left(\frac{\partial c_{\mathrm{sw}}}{\partial t} \right) \tag{1}$$

The last term in the right-hand side of Eq. (1) accounts for the amount of bound water that could possibly be desorbing from the solute matrix during primary drying; as was indicated above, the total amount of water being desorbed from the solute matrix during the primary drying stage has been shown to be negligible [10,11,14]. The concentration, c_{sw}, of bound water has units of kg water/kg solid and, therefore, the parameter ρ_{I} in Eq. (1) represents the density of the solid in the dried layer I (see Eq. (15) in this work). For the physical parameters ρ_{Ie}, c_{pIe}, and k_{Ie} of the dried layer I, effective parameters are considered based on volume-averaging theory [37] to describe the physical properties of the gas and solid phases [10,11], and the expressions for estimating the values of k_{Ie} and the term $\rho_{\mathrm{Ie}} c_{\mathrm{pIe}}$ in Eq. (1) are given in Table 1. The variable $N_{\mathrm{t,I}}$ represents the total mass flux vector ($N_{\mathrm{t,I}} = N_{\mathrm{w,I}} + N_{\mathrm{in,I}}$) which is equal to the sum of the mass flux vectors of water vapor and inerts (e.g., air). The constitutive equations used in this work for the mass flux vectors $N_{\mathrm{w,I}}$ and $N_{\mathrm{in,I}}$ are from the dusty-gas model [10–12,14,38–41] and their form for the water and inert (e.g., air) gas species present in the pores of the dried layer I are:

Table 1
Expressions and values of the physical parameters

$c_{\mathrm{pd,s}} = 2590$ J/kg K
$c_{\mathrm{pf,s}} = 1930$ J/kg K
$c_{\mathrm{pg}} = 1616.6$ J/kg K
$c^{\mathrm{o}}_{\mathrm{sw}} = 0.6415$ kg water/kg solid
$(D_{\mathrm{w,in}})_i = (4.342 \times 10^{-6}(T_i^{2.334}))/P_i$ m^2/s for $i =$ I, II
$k_{\mathrm{I,e}} = (1-\varepsilon_{\mathrm{pb}})^{1.5}[2.596 \times 10^{-4}(P_{\mathrm{I}}\|_{x=0} + P_{\mathrm{I}}\|_{x=X}) + 0.039806]$ W/m K
$k_{\mathrm{des}} = 6.48 \times 10^{-7}$ s^{-1} during the primary drying stage
$k_{\mathrm{des}} = 7.8 \times 10^{-5}$ s^{-1} during the secondary drying stage
$k_{\mathrm{d,s}} = 2.596 \times 10^{-4}(P_{\mathrm{II}}\|_{x=X} + P_{\mathrm{II}}\|_{x=L}) + 0.039806$ W/m K
$k_{\mathrm{f,s}} = 2.56$ W/m K
$L = 0.01$ m
$M_{\mathrm{in}} = 28.82$ kg/kmol
$M_{\mathrm{w}} = 18.00$ kg/kmol
$P^{\mathrm{o}}_i = 5.07$ Pa, at $t = 0$ and $0 \leqslant x \leqslant L$ for $i =$ I, II
$p^{\mathrm{o}}_{\mathrm{in,i}} = 4.00$ Pa, at $t = 0$ and $0 \leqslant x \leqslant L$ for $i =$ I, II
$p^{\mathrm{o}}_{\mathrm{w,i}} = 1.07$ Pa, at $t = 0$ and $0 \leqslant x \leqslant L$ for $i =$ I, II
$R_{\mathrm{g}} = 8.314$ J/K mol
$T_{\mathrm{lp}} = T_{\mathrm{up}} = 253.15$ K for primary drying stage
$T_{\mathrm{lp}} = T_{\mathrm{up}} = 293.15$ K for secondary drying stage
$T_{\mathrm{m}} = 263.15$ K
$T_{\mathrm{scor}} = 313.15$ K
$T^{\mathrm{o}}_i = 233.15$K, at $t = 0$ and $0 \leqslant \times \leqslant L$ for $i =$ I, II
$\Delta H_{\mathrm{s}} = 2687.4 \times 10^3$ J/kg
$\Delta H_{\mathrm{v}} = 2840 \times 10^3$ J/kg
$\varepsilon_{\mathrm{p}} = 0.785$
$\varepsilon_{\mathrm{pb}} = 0.50$
$\mu_{\mathrm{mx}} = 18.4558 \times 10^{-7}[T_i^{1.5}/(T_i + 650)]$kg/m s for $i =$ I, II
$\rho_{\mathrm{d,s}} = 328[(1 + c_{\mathrm{sw}})/(1 + c^{\mathrm{o}}_{\mathrm{sw}})]$ kg/m^3
$\rho_{\mathrm{d,s,f}} = 199.817$ kg/m^3
$\rho_{\mathrm{f,s}} = 1030$ kg/m^3
$\rho_{\mathrm{Ie}} c_{\mathrm{pIe}} \cong (1-\varepsilon_{\mathrm{pb}}) \rho_{\mathrm{d,s}}\, c_{\mathrm{pd,s}}$
$\tau_{\mathrm{I}} = \sqrt{2}$ dimensionless
$\tau_{\mathrm{II}} = \sqrt{2}$ dimensionless

$$N_{\mathrm{w,I}} = -\frac{M_{\mathrm{w}}}{R_{\mathrm{g}} T_{\mathrm{I}}} \left(k_{1,\mathrm{I}} \nabla p_{\mathrm{w,I}} + k_{2,\mathrm{I}} p_{\mathrm{w,I}} \nabla P_{\mathrm{I}} \right) \tag{2}$$

$$N_{\mathrm{in,I}} = -\frac{M_{\mathrm{in}}}{R_{\mathrm{g}} T_{\mathrm{I}}} \left(k_{3,\mathrm{I}} \nabla p_{\mathrm{in,I}} + k_{4,\mathrm{I}} p_{\mathrm{in,I}} \nabla P_{\mathrm{I}} \right) \tag{3}$$

The expressions for $k_{1,\mathrm{I}}$, $k_{2,\mathrm{I}}$, $k_{3,\mathrm{I}}$, and $k_{4,\mathrm{I}}$ are presented in the nomenclature of this paper; these parameters account for the transport of water vapor and inerts in the dried layer I by Darcy's flow (viscous flow), Knudsen diffusion, and bulk binary diffusion; the total pressure, P_{I}, in Eqs. (2) and (3) is equal to the sum of $p_{\mathrm{w,I}}$ and $p_{\mathrm{in,I}}$ ($P_{\mathrm{I}} = p_{\mathrm{w,I}} + p_{\mathrm{in,I}}$). The dusty-gas model has the major advantage of not requiring detailed information [38–41] about the porous structure of the dried layer I; if one has a rather detailed information of the pore structure of the dried layer I obtained from high-resolution optical microscopy [42–44] methods, then pore network theory [27–29] could be used to determine even more accurately the transport of heat and mass in the porous dried layer I. An estimate for the value of Darcy's flow permeability, C_{01} could be obtained from the Blake–Kozeny correlation [21]

$$C_{01,\mathrm{I}} \cong \frac{\varepsilon_{\mathrm{pb}}^3}{150(1-\varepsilon_{\mathrm{pb}})^2} d_{\mathrm{p}}^2 \tag{4}$$

where d_{p} denotes the diameter of the frozen particles that were packed on the tray or in vial forming a packed bed of particles, and $\varepsilon_{\mathrm{pb}}$ represents the porosity of the formed packed bed. It is important to note here that experimental evidence [1–4,6,8] indicates that the dimensional change of the spray frozen particles during primary and secondary drying is so small that it can be neglected, and, therefore, the value of d_{p} used in Eq. (4) can be considered to be approximately equal to the value of the diameter of the frozen particles that were packed to form a packed bed before primary drying started. This experimental evidence also indicates that the particle size (diameter) can be directly controlled by changing the atomizing conditions and, furthermore, since there is

minimal change in the particle diameter, d_p, during drying, the macroporosity ε_{pb} of the dried layer I will be approximately equal to the porosity ε_{pb} of the partially saturated porous frozen layer II formed from the packing of the frozen particles whose diameter is d_p. The macroporosity, ε_{pb}, of the dried layer I can interact with the porosity, ε_p, of the dried porous particles (after the ice has sublimated from a frozen particle, the particle acquires a porous structure whose solid material is comprised of the solute of interest and on the matrix of the solute there is bound (sorbed) water), but the effects of heat and mass transfer resistance within the porous particles are considered to be negligible because the size (diameter) of the particles used in the production of pulmonary aerosols is small (11–18 μm) and, therefore, since the size of the characteristic dimension of the particles is significantly much smaller than the size of the characteristic dimension of the packed bed formed by the packing of the particles, the lengths of the conductive pathways for heat and mass transfer within the porous particles will be substantially much smaller than the lengths of the conductive pathways for heat and mass transfer in the packed bed. But, of course, it is worth mentioning here that one could consider the heat and mass transfer resistances within the particles by employing the modeling approach for heat and mass transfer in porous particles presented in References [20,27,40,41] and, therefore, one could then quantitatively ascertain their relative effect to the overall heat and mass transfer resistances in the packed bed; it is important to indicate that, in this case, a moving sublimation interface that separates the porous dried layer surrounding the ice core of each particle will have to be considered (in addition to the moving sublimation interface that separates the porous dried layer I from the porous frozen layer II, as per Fig. 1, and the energy and material balances at this moving sublimation interface are presented in Eqs. (25) and (26) of this work) and this will significantly complicate the structure of the mathematical model as well as its solution. The mean pore diameter, d_{pore}, formed from the packing of the particles can be estimated from the hydraulic diameter [21] as follows:

$$d_{pore} = \left(\frac{1}{3}\right)\left(\frac{\varepsilon_{pb}}{1-\varepsilon_{pb}}\right)d_p \tag{5}$$

It should be noted here that in spray freeze drying, as Eq. (5) indicates, the mean size of the pores of the packed bed formed from the packing of the particles of the material in a container (tray or vial), is determined by the particle diameter, d_p, and the packing porosity, ε_{pb}, and, for instance, if $\varepsilon_{pb} = 0.50$ and $d_p = 15$ μm, then the value of d_{pore} from Eq. (5) is about 5 μm. But this mean pore size is significantly smaller than the mean pore size encountered in the dried layer of a material undergoing conventional freeze drying where the pores of the dried layer [14] depend on the size of the ice crystals which can grow even larger than 50 μm due to the slow freezing rates [14,15] that can be employed in the freezing stage of conventional freeze drying; furthermore, the mass transfer resistance of solution based materials (conventional freeze drying) can be further reduced by an annealing process employed before the start of the primary drying stage. However, the size of the pores, d_{pore}, of the porous frozen layer II of particle based materials is determined by the particle size, d_p, and the packing porosity, ε_{pb}, and, furthermore, the annealing procedure has little effect on the pore diameter, d_{pore}. The fact that the pores of the dried layer in conventional freeze drying can be significantly larger than those in spray freeze drying, would suggest that the mass transfer resistance in the dried layer of a material undergoing spray freeze drying is larger than that would be encountered in the dried layer of the same material undergoing conventional freeze drying, considering, of course, that the pore connectivity [27–29,43] of the porous material for both solution based freeze drying (conventional freeze drying) and particle based freeze drying (spray freeze drying) is high. It is very important to emphasize that even if the pores of a porous medium are large, the resistance to mass transfer could be high if the pore connectivity [27–29,43] is low. The removal of bound water is modeled by the following expression [10,11,14]:

$$\frac{\partial c_{sw}}{\partial t} = -k_{des}c_{sw} \tag{6}$$

As discussed earlier, the porosity of the particles, ε_p, resulting after the primary drying stage of the packed frozen particles has been completed, is determined by the initial formulation of the solution, while the porous structure of the packed bed of frozen particles is defined by the packing porosity ε_{pb} and the particle diameter d_p. The porous frozen layer II is partially saturated and the ice saturation, S (the symbol S for denoting the ice saturation and used by Wang and Shi [25] is also employed here but its definition is different than that in Reference [25] because the system studied in this work is very different than that examined by Wang and Shi [25]) is defined here as the fraction of the ice volume to the pore volume in the particle

$$S = \frac{\frac{4}{3}\varepsilon_p\pi d_{ice}^3}{\frac{4}{3}\varepsilon_p\pi d_p^3} = \left(\frac{d_{ice}}{d_p}\right)^3 \tag{7}$$

where the parameter d_{ice} represents the diameter of an ice core in the particle that becomes smaller as drying proceeds. In other words, the ice core of the particle is surrounded by a porous dried layer and the size d_{ice} of the ice core decreases with time as drying proceeds. It should be noted here that the thermal conductivity of the dried porous layer $(d_p - d_{ice})$ that surrounds the ice core is significantly lower than the thermal conductivity of the frozen solution in the ice core, but because the characteristic dimension of the particles is substantially much smaller than the characteristic dimension of the packed bed formed by the packing of the frozen particles, the conductive pathways in the particles for mass and heat transfer are substantially much smaller than those in the packed bed and, thus, the resistances for heat and mass transfer in the individual particles are considered to be negligible relative to those in the packed bed, as discussed earlier. The energy balance in the porous frozen layer II is given by Eq. (8)

$$\rho_{II}c_{pII}\left(\frac{\partial T_{II}}{\partial t}\right) = \nabla\cdot(k_{II}\nabla T_{II}) - c_{pg}(\nabla\cdot(N_{t,II}T_{II})) + \Delta H_s(\rho_f - \rho_d)\frac{\partial S}{\partial t} + \Delta H_v\rho_I\left(\frac{\partial c_{sw}}{\partial t}\right) \tag{8}$$

By using a volume-averaging approach [37,45], the parameters ρ_{II}, $\rho_{II}c_{pII}$, ρ_f, ρ_d, $\rho_{d,s}$, ρ_I, and k_{II} can be determined from the following expressions:

$$\rho_{II} \cong S_{av}\rho_f + (1-S_{av})\rho_d \cong (1-\varepsilon_{pb})\left(S_{av}\rho_{f,s} + (1-S_{av})\rho_{d,s}\right) \tag{9}$$

$$\rho_{II}c_{pII} \cong S_{av}\rho_f c_{pf} + (1-S_{av})\rho_d c_{pd} \cong (1-\varepsilon_{pb})\left(S_{av}\rho_{f,s}c_{pf,s} + (1-S_{av})\rho_{d,s}c_{pd,s}\right) \tag{10}$$

$$k_{II} \cong S_{av}k_f + (1-S_{av})k_d \cong S_{av}(1-\varepsilon_{pb})^{1.5}k_{f,s} + (1-S_{av})(1-\varepsilon_{pb})^{1.5}k_{d,s} \tag{11}$$

$$\rho_f = (1-\varepsilon_{pb})\rho_{f,s} \tag{12}$$

$$\rho_d = (1-\varepsilon_{pb})\rho_{d,s} \tag{13}$$

$$\rho_{d,s} = (1+c_{sw})\rho_{d,s,f} \tag{14}$$

$$\rho_I = (1-\varepsilon_{pb})\rho_{d,s,f} \tag{15}$$

In Eqs. (9)–(13), S_{av} represents the volume-averaged ice saturation $(0 \leqslant S_{av} \leqslant 1)$ given by Eq. (16)

$$S_{av} = \left(\frac{1}{V_{II,p}}\right)\int_0^{V_{II,p}} S dV_{II,p} \tag{16}$$

where $V_{II,p}$ represents the volume of the porous frozen region II occupied by the particles. Furthermore, (i) ρ_f and ρ_d denote the apparent density of a frozen particle based material ($S_{av} = 1$) and of a dried particle based material after primary drying ($S_{av} = 0$), respectively, (ii) c_{pf} and c_{pd} represent the apparent heat capacities of a frozen ($S_{av} = 1$) and dried ($S_{av} = 0$) particle based material, respectively, (iii) k_f and k_d are the apparent thermal conductivities of a frozen ($S_{av} = 1$) and dried ($S_{av} = 0$) particle based material, respectively, (iv) $\rho_{f,s}$ and $\rho_{d,s}$ represent the densities of frozen and dried solution based material, respectively, (v) $\rho_{d,s,f}$ is the density of the solution based material when it is fully dried and both forms of frozen and sorbed water have been removed, (vi) $c_{pf,s}$ and $c_{pd,s}$ denote the heat capacities of frozen and dried solution based material, respectively, and (vii) $k_{f,s}$ and $k_{f,d}$ are the thermal conductivities of frozen and dried solution based material, respectively. In Eq. (8) the amount of energy used to remove bound (sorbed) water from the matrix of the solute in the particles is considered, but the amount of sorbed water removed during primary drying from the matrix of the solute in the porous frozen layer II is usually negligible. Also, from Eq. (11) it can be observed that the value of the thermal conductivity, k_{II}, of the porous frozen layer II can be significantly lower than the thermal conductivity, $k_{f,s}$, of the frozen solution based material, and, thus, the conduction of heat in the porous frozen layer II of a material undergoing spray freeze drying could be substantially lower than the conduction of heat in the frozen solution of the material undergoing conventional freeze drying . The total mass flux $N_{t,II}$ of water vapor and inerts ($N_{t,II} = N_{w,II} + N_{in,II}$) can be determined from Eqs. (17) and (18)

$$N_{w,II} = -\frac{M_w}{R_g T_{II}}\left(k_{1,II}\nabla p_{w,II} + k_{2,II} p_{w,II}\nabla P_{II}\right) \tag{17}$$

$$N_{in,II} = -\frac{M_{in}}{R_g T_{II}}\left(k_{3,II}\nabla p_{in,II} + k_{4,II} p_{in,II}\nabla P_{II}\right) \tag{18}$$

The reason that the parameters $k_{1,II}$, $k_{2,II}$, $k_{3,II}$, and $k_{4,II}$, have different values in the porous frozen layer II than the values of the parameters $k_{1,I}$, $k_{2,I}$, $k_{3,I}$, and $k_{4,I}$ of the porous dried layer I is due to the fact that the temperature, the total pressure, and the partial pressures of water vapor and inerts are different in the two porous layers.

The continuity equations for the water vapor and the inert gas (e.g., air) in the pores of the porous dried (I) and porous frozen (II) layers have the following forms:

$$\frac{\varepsilon_{t,I} M_w}{R_g T_I}\left(\frac{\partial p_{w,I}}{\partial t}\right) = -\nabla\cdot N_{w,I} - \rho_I \frac{\partial c_{sw}}{\partial t} \tag{19}$$

$$\frac{\varepsilon_{t,I} M_{in}}{R_g T_I}\left(\frac{\partial p_{in,I}}{\partial t}\right) = -\nabla\cdot N_{in,I} \tag{20}$$

$$\frac{M_w}{R_g T_{II}}\left(\frac{\partial\left(\varepsilon_{t,II} p_{w,II}\right)}{\partial t}\right) = -\nabla\cdot N_{w,II} - (\rho_f - \rho_d)\frac{\partial S}{\partial t} - \rho_I \frac{\partial c_{sw}}{\partial t} \tag{21}$$

$$\frac{M_{in}}{R_g T_{II}}\left(\frac{\partial\left(\varepsilon_{t,II} p_{in,II}\right)}{\partial t}\right) = -\nabla\cdot N_{in,II} \tag{22}$$

The total pressure, P_{II}, in Eqs. (17) and (18) is equal to the sum of $p_{w,II}$ and $p_{in,II}$, ($P_{II} = p_{w,II} + p_{in,II}$). In Eq. (21), the value of ice saturation, S, is greater than zero ($S > 0$) and, therefore, the pressure of water vapor, $p_{w,II}$, in the porous frozen layer II is directly determined from the saturated water vapor pressure $p_w^{sat}(T_{II})$. Marti and Mauersberger [46] have provided an expression for $p_w^{sat}(T)$ based on new measurements of ice vapor pressures at temperatures between 170 K and the triple point of water which is as follows:

$$p_{w,II} = p_w^{sat}(T_{II}) = 10^{(-2663.5/T_{II})+12.537} \tag{23}$$

Therefore, for values of $S > 0$, the term $\partial p_{w,II}/\partial t$ in Eq. (21) could be determined from the expression

$$\frac{\partial p_{w,II}}{\partial t} = \frac{dp_w^{sat}}{dT_{II}}\frac{\partial T_{II}}{\partial t} \tag{24}$$

where the term $\partial T_{II}/\partial t$ is determined from the solution of Eq. (8). The evolution of ice saturation, S, is then determined from the solution of Eq. (21) which states that the change in the value of ice saturation, S, with time in a finite volume element of the porous frozen layer II is equal to the sum of the water vapor that leaves the volume element and the change in the water vapor that is contained in the volume element. If the value of ice saturation, S, at a certain time and local position within the porous frozen layer II becomes greater than one ($S > 1$), this would indicate that water vapor produced by sublimation near the bottom, L, of the sample due to heat supplied by the lower heating plate (see Fig. 1), would have been redistributed by transport in the porous frozen layer II and at that certain time and local position in the porous frozen layer II the local temperature T_{II} would have been such that the water vapor could have been condensed and considered to be deposited as ice around the particles. In Eqs. (19) and (20), $\varepsilon_{t,I}$ represents the total porosity of the dried layer I which is obtained from the expression

$$\varepsilon_{t,I} = \varepsilon_{pb} + (1 - \varepsilon_{pb})\varepsilon_p \tag{25}$$

In Eqs. (21) and (22), $\varepsilon_{t,II}$ represents the total porosity of the porous frozen layer II and its value varies with time because the value of the volume-averaged ice saturation, S_{av}, varies with time, and, therefore, the porosity, $\varepsilon_{p,II}$, in the particles of the porous frozen layer II varies with time. The values of $\varepsilon_{p,II}$ and $\varepsilon_{t,II}$ can be determined from the following expressions:

$$\varepsilon_{p,II} = \varepsilon_p(1 - S_{av}) \tag{26}$$

$$\varepsilon_{t,II} = \varepsilon_{pb} + (1 - \varepsilon_{pb})\varepsilon_{p,II} = \varepsilon_{pb} + (1 - \varepsilon_{pb})\varepsilon_p(1 - S_{av}) \tag{27}$$

Therefore, at the end of primary drying $S_{av} = 0$ and $\varepsilon_{t,II}$ will be equal to $\varepsilon_{t,I}$.

An energy balance at the moving sublimation interface ($x = X$ for planar geometry involving bulk spray freeze drying on trays and $z = Z = H(t,r)$ for spray freeze drying in vials on trays [10,11,14], as per Fig. 1a and b, respectively) whose thickness is taken to be infinitesimal [10,11,14] gives

$$-(-k_{II}\nabla T_{II})\cdot n_{interf} + (-k_{Ie}\nabla T_I)\cdot n_{interf} + \left(\rho_{II} c_{pII} T_{II} - \rho_I c_{pI} T_I\right) V\cdot n_{interf} + c_{pg} T_{interf} N_{t,\,interf} = -\Delta H_s N_{w,interf} \tag{28}$$

In Eq. (28), n_{interf} denotes the normal vector to the moving sublimation interface, T_{interf} denotes the temperature of the interface ($T_{interf} = T_I = T_{II}$ at the moving sublimation interface), $N_{w,interf}$ is the mass flux of water vapor at the moving interface, $N_{t,interf}$ is the total mass flux of water vapor and inerts at the moving interface, and V denotes the velocity of the moving interface. A material balance at the moving interface defines the velocity, V [10,11,14], and gives

$$V = -\frac{N_{w,interf}}{\rho_{II} - \rho_I} \qquad \text{at the moving interface for } t \geqslant 0 \tag{29}$$

If $N_{w,I}|_{interf^-}$ represents the mass flux of water vapor in the dried layer I immediately above the moving interface and $N_{w,II}|_{interf^+}$ denotes the mass flux of water vapor in the porous frozen layer II immediately below the interface, then a water vapor mass balance at the moving sublimation front would give

$$N_{w,I}|_{interf^-} - N_{w,II}|_{interf^+} = N_{w,interf} \quad \text{for } t \geqslant 0 \tag{30}$$

In order to quantify the contributions of $N_{w,I}|_{interf^-}$ and $N_{w,II}|_{interf^+}$ to the drying rate per unit surface area, a new parameter ζ is defined as

$$\zeta = \frac{N_{w,II}|_{interf^+}}{N_{w,I}|_{interf^-}} \tag{31}$$

where ζ represents the influence of sublimation phenomena in the porous frozen layer II on heat and mass transfer during the primary drying stage.

The initial and boundary conditions for Eqs. (1), (6), (8), (19), (20), and (29) for the cases of (a) bulk spray freeze drying on trays, and (b) spray freeze drying in vials on trays, can be found in References [10–12,14,47] because the initial and boundary conditions for the above mentioned equations of spray freeze drying have the same form and structure as those employed in conventional freeze drying . The initial and boundary conditions for Eqs. (21) and (22) which provide the evolution of the ice saturation, S, and the time varying distribution of the partial pressure, $p_{in,II,}$ of the inerts (e.g., air) in the pores of the porous frozen layer II (the time varying distributions of the partial pressure of water vapor, $p_{w,II}$, in the pores of the porous frozen layer II is determined from Eqs. (23) and (24)), respectively, are as follows:

$$\text{at } t = 0, S = 1 \text{ everywhere in the porous frozen layer II} \tag{32}$$

$$\text{at } t = 0, p_{in,II} = p^{o}_{in,II} \text{ everywhere in the porous frozen layer II} \tag{33}$$

$$\text{at impermeable surfaces,} \quad \nabla p_{in,\,II} = 0, \text{ for } t \geqslant 0 \tag{34}$$

$$\text{at a centerline of symmetry,} \nabla p_{in,\,II} = 0, \text{ for } t \geqslant 0 \tag{35}$$

Eqs. (1)–(29) and (32)–(35) represent the mathematical model that could be used to describe the dynamic behavior of the primary drying stage of spray freeze drying. It is very important to indicate here that the control variables represented by the heat inputs q_I and q_{II} and the pressure in the drying chamber P_{dcham} [10–12,14,47] have to have dynamic values during the primary drying stage such that (i) the temperature, T_{interf}, of the moving interface and the temperature, T_{II}, in the region of the porous frozen layer II having $S > 0$ are always less [10–12,14] than the melting temperature T_m of the frozen material (T_m represents the glass temperature for amorphous formulations while for totally crystalline formulations T_m represents the eutectic temperature), and (ii) the temperature, T_I, in the porous dried layer I and the temperature, T_{II}, in the porous frozen layer II having $S = 0$ are always less than the scorch temperature, T_{scor}, of the dried material [10–12,14]. Also, the model presented in this section could be used to describe the dynamic behavior of the primary drying stage of a process involving the drying of frozen particles in packed beds.

2.2. Mathematical model for the secondary drying stage of spray freeze drying

During the secondary drying stage, there is no longer a porous frozen layer II present, and the transport equations now concern only T_I, $p_{w,I}$, and $p_{in,I}$ in the porous dried layer I; during the secondary drying stage, bound (sorbed) water is removed from the matrix of the solute in the porous dried layer I and the end of the secondary drying stage occurs when the average concentration of bound water in the matrix of the solute has reached a desirable value so that the stability and quality of bioactivity of the dried material of interest will remain high for a long period of time [10–12,14,47]. Furthermore, since during the secondary drying stage there is present only the porous dried layer I, it is apparent that there is no moving sublimation interface because there is no longer a porous frozen layer II in the material being dried. The energy and material balance equations in the dried layer I during the secondary drying stage, are given by Eqs. (1), (6), (19) and (20). The initial conditions for Eqs. (1), (6), (19) and (20) are given by the spatial profiles of T_I, c_{sw}, $p_{w,I}$ and $p_{in,I}$, respectively, at the end of the primary drying stage [10–12,14,47]. The boundary conditions for Eqs. (1), (6), (19) and (20) for the cases of (a) bulk spray freeze drying on trays, and (b) spray freeze drying in vials on trays, can be found in References [10–12,14,47] because the boundary conditions for Eqs. (1), (6), (19) and (20) have the same form and structure as those employed in conventional freeze drying.

Eqs. (1), (6), (19) and (20) represent the mathematical model that could be used to describe the dynamic behavior of the secondary drying stage of spray freeze drying. It should be indicated here that the control variables q_I, q_{II}, and P_{dcham} have to have dynamic values during the secondary drying stage such that the temperature, T_I, everywhere in the porous dried layer I is kept below the value of the scorch temperature, T_{scor}, of the dried material [10–12,14,47]. Furthermore, the model presented in this section could be used to describe the dynamic behavior of the secondary drying stage of a process involving the drying of frozen particles in packed beds.

3. Results and discussion

The mathematical model constructed and presented in Sections 2.1 and 2.2 of this work was numerically solved through the use of the method of orthogonal collocation [10,11] and simulation results are presented in this work for the spray freeze drying of skim milk on trays, as per Fig. 1a; skim milk was selected because it could be considered as a complex pharmaceutical product in the sense that it contains enzymes and proteins [10–14]. The values of the parameters $C_{01,i}$, $C_{1,i}$, and $C_{2,i}$ (i = I, II) that are required for the determination of the dusty-gas [10–14,38–41] variables $k_{1,i}$, $k_{2,i}$, $k_{3,i}$, and $k_{4,i}$ (i = I, II) in the porous dried layer I and in the porous frozen layer II are estimated from the following expressions:

$$C_{01,i} \cong C_{01,II} \cong \frac{\varepsilon_{pb}^3}{150(1-\varepsilon_{pb})^2} d_p^2 \tag{36}$$

$$C_{1,I} \cong \frac{(\varepsilon_{t,I}/\tau_I)48.5 d_{pore}}{R_g^{0.5}} = \frac{\left((\varepsilon_{pb} + (1-\varepsilon_{pb})\varepsilon_p)/\sqrt{2}\right)48.5 d_{pore}}{R_g^{0.5}} \tag{37}$$

$$C_{1,II} \cong \frac{(\varepsilon_{t,II}/\tau_{II})48.5 d_{pore}}{R_g^{0.5}} = \frac{\left((\varepsilon_{pb} + (1-\varepsilon_{pb})\varepsilon_p)(1-S_{av})/\sqrt{2}\right)48.5 d_{pore}}{R_g^{0.5}} \tag{38}$$

$$C_{2,I} \cong \frac{\varepsilon_{t,\,I}}{\tau_I} = \frac{(\varepsilon_{pb} + (1-\varepsilon_{pb})\varepsilon_p)}{\sqrt{2}} \tag{39}$$

$$C_{2,II} \cong \frac{\varepsilon_{t,\,II}}{\tau_{II}} = \frac{(\varepsilon_{pb} + (1-\varepsilon_{pb})\varepsilon_p(1-S_{av}))}{\sqrt{2}} \tag{40}$$

In Eqs. (37)–(40), the parameters τ_I and τ_{II} denote the tortuosity factor for the porous dried layer I and the porous frozen layer II, respectively, and the value of the tortuosity factor for both layers is taken to be equal to $\sqrt{2}$ which could provide a reasonable approximation [40,41,48,49] for the value of the tortuosity factor for random porous structures whose pores have relatively good pore connectivity. The value of d_{pore} in Eqs. (37) and (38) is estimated from Eq. (5). The values as well as the expressions by which

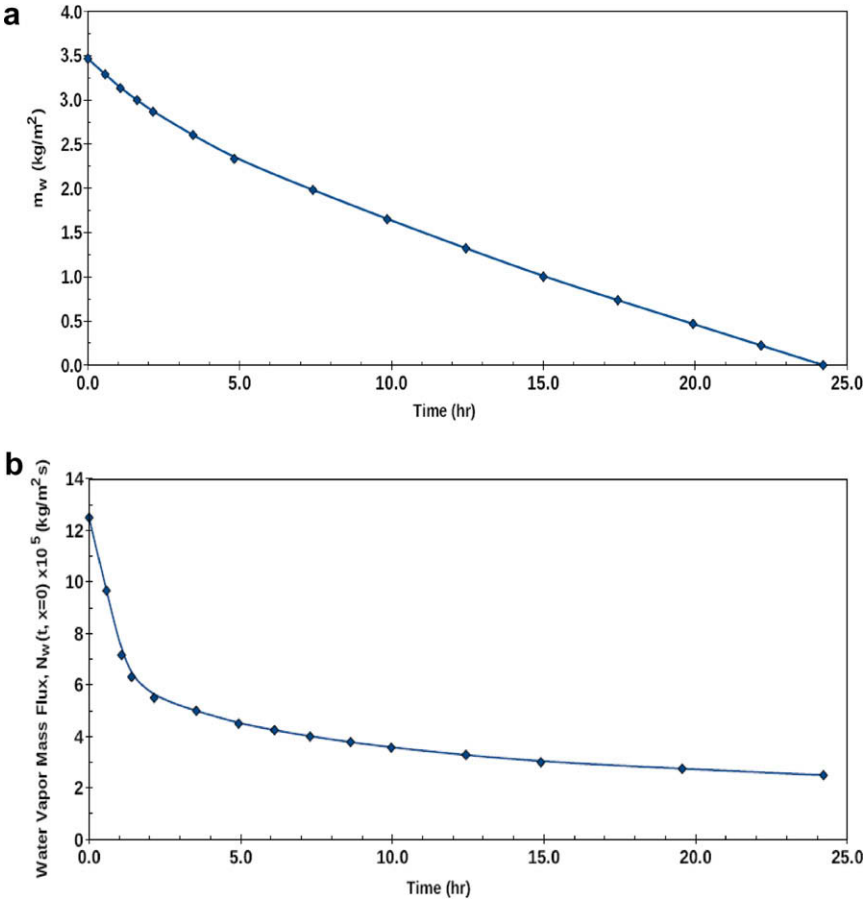

Fig. 2. Drying behavior during the primary drying stage of spray freeze drying when L = 1.0 cm, d_p = 15 μm, and ε_{pb} = 0.5. (a) Drying curve. (b) Drying rate.

the values of the remaining parameters of the model presented in Section 2 are determined, can be found in Table 1 of Reference [10], Table 1 of Reference [11], and in Table 1 of this work.

In Fig. 2a, the amount of free water, m_w, in the material (in units of kg/m^2) versus time, t, is presented (drying curve) and in Fig. 2b the mass flux, N_w (t,x = 0), of free water at x = 0 versus time, t, is shown (drying rate) during the primary drying stage of spray freeze drying with the value of the porosity of the packed bed of particles, ε_{pb}, being equal to 0.5 (see Table 1). The results in Fig. 2 show that it takes 24.214 h to complete the primary drying stage of the spray freeze drying system whose parameter values are given in Table 1. The completion of the primary drying stage of the conventional freeze drying of the solution based (ε_{pb} = 0) skim milk requires 26.064 h. But since the value of ε_{pb} is equal to 0.5 in the case of the freeze drying system considered here, the amount of free water to be removed from the particle based skim milk system by sublimation of ice is about 50% of that removed in the solution based skim milk system, and, therefore, this result clearly indicates that the spray freeze drying of a given product whose thickness in the tray is L would require significantly larger drying times for the removal of free water by sublimation of ice than the conventional freeze drying of the same product whose thickness in the tray is the same as that in the spray freeze drying system. One major reason for the substantial reduction in the primary drying rate in spray freeze drying is the fact that the heat transfer rate in the particle based material is reduced due to the significant reduction in the value of the effective thermal conductivity, k_{II}, as can be seen from Eq. (11). For the case where ε_{pb} = 0.5 and at the start of the primary drying stage (t = 0) when S_{av} = 1.0, the value of k_{II} for the particle based material is about 63% of the value of the thermal conductivity, $k_{f,s}$, of the frozen solution based material, while when the value of S_{av} = 0.5 the value of k_{II} is only about 32% of the value of $k_{f,s}$; of course as the primary drying stage proceeds and $S_{av} \to 0$, the value of k_{II} will become about equal to 63% of the value of the thermal conductivity, $k_{d,s}$, of the dried solution based material which is only about 2% of the value of $k_{f,s}$. Furthermore, the drying rate in Fig. 2b of the particle based material is about half that of the solution based [10] material and also decreases more rapidly with time. This finding would suggest that the mass transfer resistance of a particle based material is substantially larger than that of a solution based material. As we discussed earlier in this work, the pore sizes of solution based materials depend on the size of the crystals formed during the freezing stage of the freeze drying process and the crystals in such systems can grow larger than 50 μm due to the slow freezing rates and the use of an annealing procedure [14,15]. But the mean pore diameter, d_{pore}, of the particle based material generated by spray freezing is determined by the particle size, d_p, and the porosity of the packing, ε_{pb}, of the particles as Eq. (5) indicates; for the particle based material considered in this work with d_p = 15 μm and ε_{pb} = 0.5, the mean pore diameter, d_{pore}, is only 5 μm. Therefore, the values of the parameters that characterize the rate of mass transfer by Darcy's flow and Knudsen and bulk diffusion (see Eqs. (2), (3), (17) and (18)) and which depend on the magnitude of the pore sizes in the material being dried, will be smaller in the case of particle based material than the values of the same parameters in the case of solution based material, and, thus, the mass transfer resistance of a particle based material will be larger than that of a solution based material.

In Fig. 3a, the temperatures at x = 0, x = X (position of moving sublimation interface), and x = L for the particle based material are plotted versus time during the primary drying stage of the

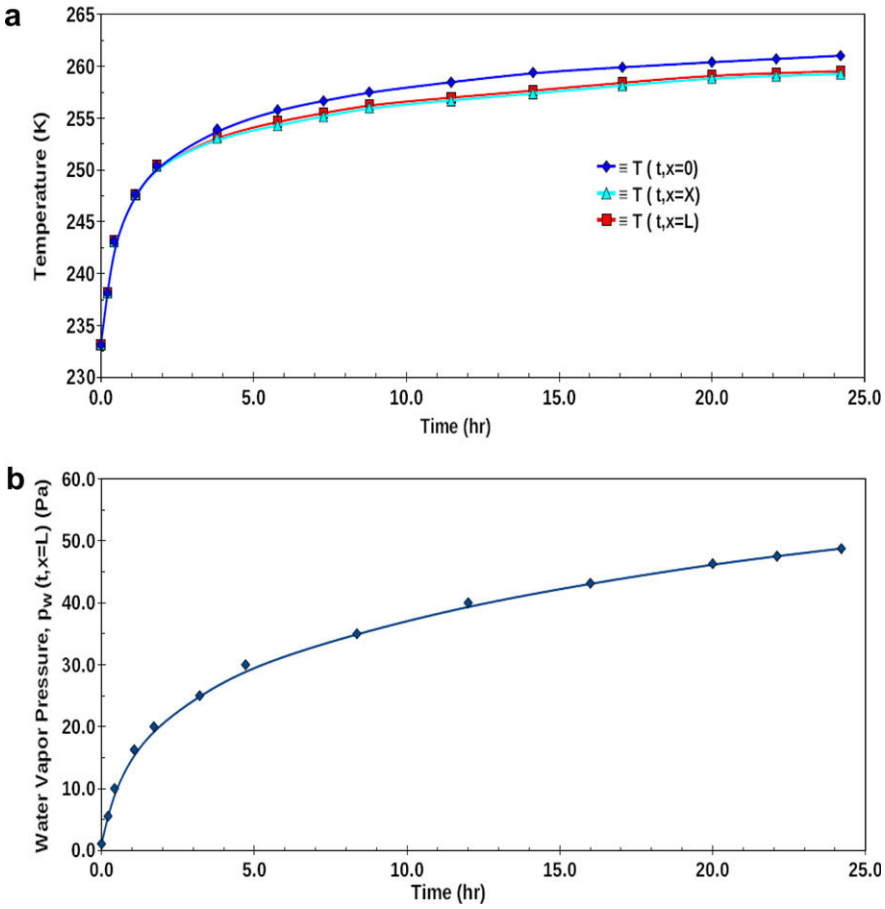

Fig. 3. Primary drying stage of spray freeze drying when $L = 1.0$ cm, $d_p = 15$ μm, and $\varepsilon_{pb} = 0.5$. (a) Dynamic behavior of temperature at positions $x = 0$, $x = X$ and $x = L$. (b) Dynamic behavior of the water vapor pressure, p_w, at position $x = L$.

spray freeze drying process. The temperature T_I $(t, x = 0)$ is highest while the temperature at the sublimation interface, $T_X = T_I$ $(t, x = X)$, is the lowest due to the consumption of energy for the sublimation of ice. But the temperature difference inside the particle based material is small, as was the case with the solution based [10] material, and less than about 3 °C throughout the primary drying stage of the spray freeze drying process. Of course, the temperature level of the solution based [10] material is substantially lower than that of the particle based product by about 10 °C and this is partially due to the higher thermal conductivity of the solution based [10] material, as was discussed above for the results in Fig. 2. In Fig. 3b, the partial pressure of water vapor at $x = L$ for the particle based material is plotted versus time during the primary drying stage of the spray freeze drying process. It can be observed that the value of $p_{w,II}(t, x = L)$ increases with time in order to overcome the increased mass transfer resistance due to the increasing with time size of the dried layer I. By recalling that the drying rate of the particle based material is about half of that of the solution based material, the mass transfer resistance of the particle based material is estimated to be about five times larger than that of the solution based material. The increased mass transfer resistance of the particle based material requires a higher water vapor pressure, $p_{w,II}$, and, of course, a higher total pressure P_{II}, for mass transfer, and this increases the temperature in the material being dried; the increased mass transfer resistance in the particle based material represents another reason (apart from the reason due to the lower thermal conductivity of the particle based material) for the higher temperature level encountered in the particle based material when compared with the temperature level obtained [10] in the solution based material.

In Fig. 4, the distribution of ice saturation, S, in the particle based material is presented at selected times during the primary drying stage of the spray freeze drying process. For times $t \geqslant 8$ h a secondary dried layer near the surface of the lower heating plate $(x \cong L)$ is being developed and the water vapor generated near the position $x \cong L$ (see Fig. 1a) is redistributed at positions $x < L$ as the deposition of ice around the particles, as is indicated by having the ice saturation attaining values greater than unity $(S > 1)$. It has been well established [10,11,14] that in freeze drying systems the primary source for the energy used in the sublimation of ice is provided from the lower heating plate by conduction through the frozen layer II. The small thermal conductivity, k_{Ie}, of the dried layer being formed above the surface of the lower heating plate and below the decreasing in size porous frozen layer II, reduces the heat transfer rate from the lower heating plate to the porous frozen layer II because $k_{Ie} \ll k_{II}$, and this prolongs the duration of the primary drying stage of the spray freeze drying process.

In Figs. 5–7 the effect of the structural parameters of product size, L, particle diameter, d_p, and packing porosity, ε_{pb}, on the duration of the primary drying stage, t_{pd}, of the spray freeze drying process are presented, respectively. The results in Fig. 5 show that as L increases the value of t_{pd} increases and, of course, a longer primary drying time results in a larger in size secondary dried layer near the bottom surface of the particle based material (as was discussed above for the results in Fig. 4), and this secondary dried layer in turn decreases the drying rate by reducing the heat transfer from the lower heating plate to the remaining porous frozen layer II. For instance, the primary drying time, t_{pd}, for $L = 5$ mm is 8.857 h, but when $L = 10$ mm the value of t_{pd} is 24.214 h, and this indicates that the duration of the primary drying stage, t_{pd}, was reduced by

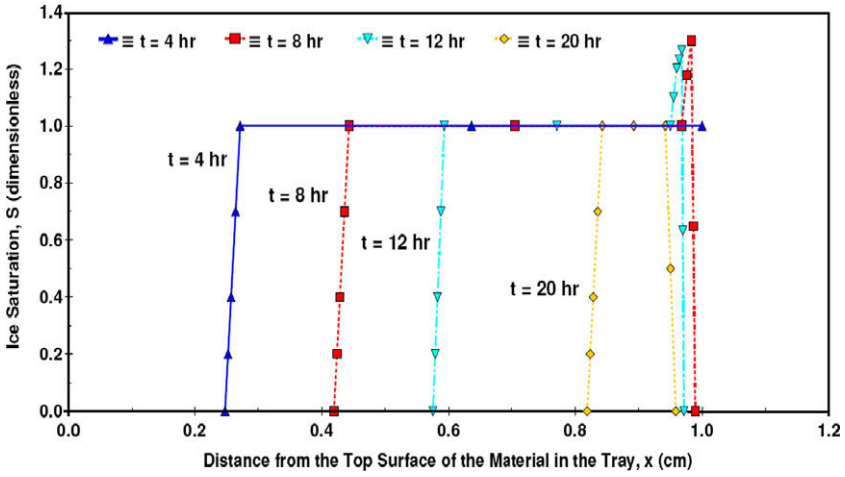

Fig. 4. The distribution of ice saturation, S, at different times during the primary drying stage of spray freeze drying when $L = 1.0$ cm, $d_p = 15$ μm, and $\varepsilon_{pb} = 0.5$.

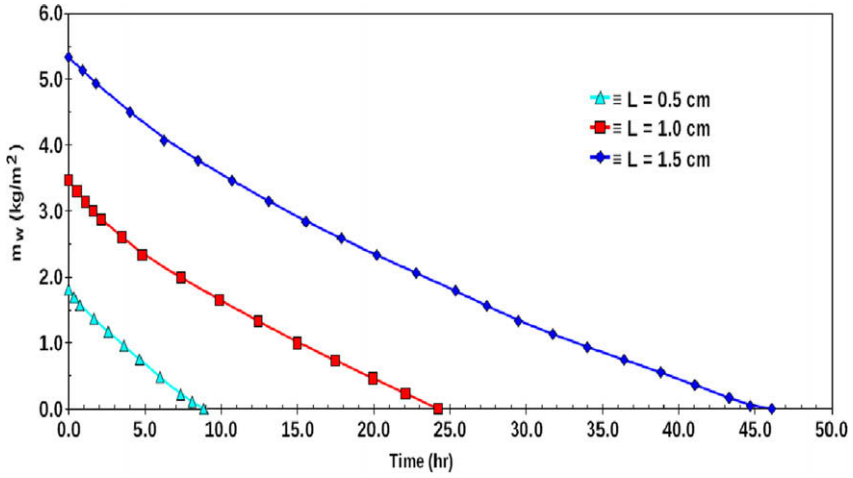

Fig. 5. The effect of product height, L, on the drying curve during the primary drying stage of spray freeze drying when $d_p = 15$ μm, and $\varepsilon_{pb} = 0.5$.

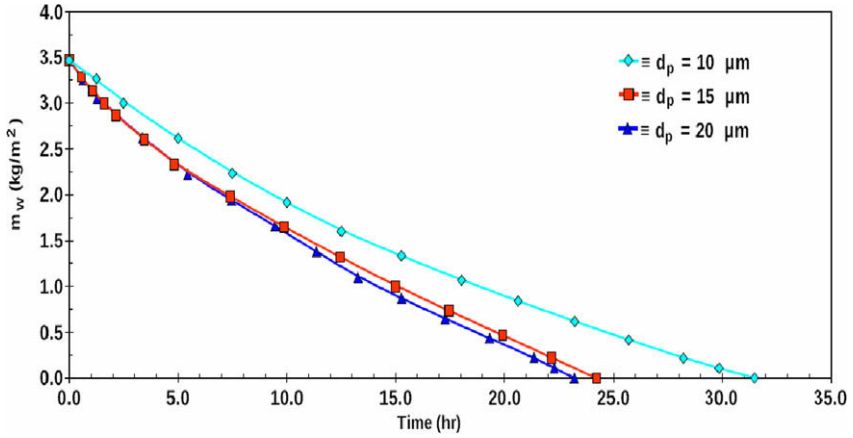

Fig. 6. The effect of particle diameter, d_p, on the drying curve during the primary drying stage of spray freeze drying when $L = 1.0$ cm and $\varepsilon_{pb} = 0.5$.

63.42% as a result of a change of the thickness, L, of the product from 10 to 5 mm; when the value of L increased from 10 to 15 mm, the value of t_{pd} was increased from 24.214 to 46.071 h indicating an increase of 90.26% in the value of t_{pd}. The results in Fig. 5 clearly indicate that the duration of the primary drying stage, t_{pd}, is a nonlinear function of the size L of the material being dried and numerous simulation results have indicated that this nonlinear effect is strongly dependent on the thickness of the secondary dried layer formed next to the surface of the lower heating plate.

In Fig. 6, it can be observed that larger diameter, d_p, particles result in a shorter duration of the primary drying stage, t_{pd}; for instance, by increasing the particle diameter from 10 to 20 μm

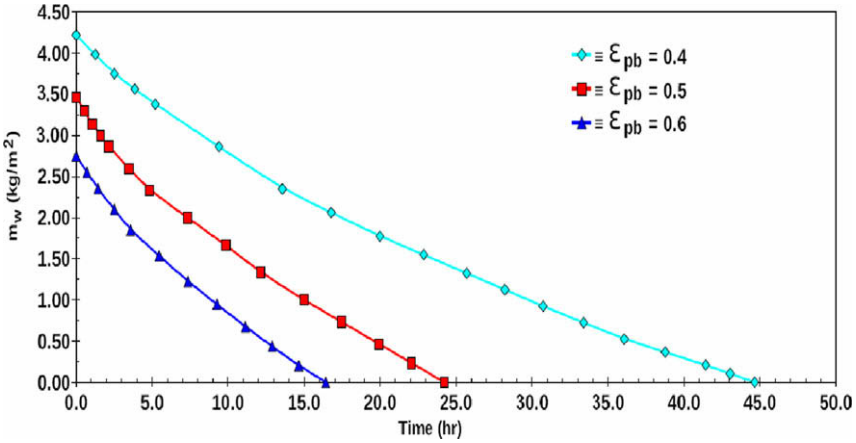

Fig. 7. The effect of packing porosity, ε_{pb}, on the drying curve during the primary drying stage of spray freeze drying when L = 1.0 cm and d_p = 15 μm.

decreases the duration of the primary drying stage, t_{pd}, from 31.071 to 22.67 h which corresponds to a reduction in the value of t_{pd} by 27.04%. It is important to indicate here that the size of the pores in the particle based material is directly dependent on the size of the particle, d_p, as is shown in Eq. (5), and, therefore, since the mean pore diameter, d_{pore}, affects the values of the parameters $C_{1,I}$ and $C_{1,II}$ (see Eqs. (37) and (38)) that characterize the Knudsen diffusivity that plays a very significant role in mass transfer at the very low pressures employed in freeze drying, the mass transfer resistance of the particle based materials becomes a function of the particle diameter, d_p. Furthermore, the values of the parameters $C_{01,I}$ and $C_{01,II}$ (see Eq. (36)) that characterize Darcy's flow (viscous flow) increase as the value of the particle diameter, d_p, increases. However, very large particle diameters which would produce very large values for d_{pore}, would not substantially enhance the mass transfer rates in particle based materials because bulk binary diffusion dominates mass transfer when the value of d_{pore} is very large and makes the Knudsen number [50] to become small in magnitude.

In Fig. 7, the effect of packing porosity, ε_{pb}, on the duration of the primary drying stage, t_{pd}, of spray freeze drying is shown. The results indicate that as the value of ε_{pb} increases the value of t_{pd} decreases and this is primarily due to the fact that the initial (t = 0) amount of frozen free water decreases as ε_{pb} increases (see Fig. 7) and also, for reasons discussed above, the drying rate is enhanced as the value of ε_{pb} increases. The effect of ε_{pb} is similar to that of the particle diameter, d_p, and larger values of ε_{pb} generally result in lower mass transfer resistance and this contributes to the increase of the drying rate.

4. Conclusions

A mathematical model that can be used to study the dynamic behavior of the primary and secondary drying stages of spray freeze drying (freeze drying of particle based materials) in trays and in vials on trays, was constructed and presented in this work. The simulation results obtained from spray freeze drying in trays indicate that reductions in the heat and mass transfer capabilities of the particle based materials are the main reasons for the longer drying times required by spray freeze drying when compared to those required by the freeze drying of solution based materials (conventional freeze drying). The development of a secondary dried layer near the surface of the lower heating plate also partially contributes to the deterioration of the drying rate during the primary drying stage of spray freeze drying. The results for spray freeze drying presented in this work, show that the drying rate during the primary drying stage increases as (i) the product height, L, decreases, (ii) the particle diameter, d_p, increases and (iii) the value of the packing porosity, ε_{pb}, increases. The mathematical model presented in this work is considered to offer a necessary and essential capability that could be used for the design, optimization, and control of the spray freeze drying process as well as of a process involving the drying of frozen particles in packed beds.

Acknowledgements

The authors are grateful to Dr. N. Markatos for his help with the simulations and for the support of this work by Criofarma-Freeze Drying Equipment, Turin, Italy.

References

[1] H.R. Costantino, L. Firouzabadian, K. Hogeland, C. Wu, C. Beganski, K.G. Carrasquillo, M. Cordova, K. Griebenow, S.E. Zale, M.A. Tracy, Protein spray-freeze drying. Effect of atomization conditions on particle size and stability, Pharm. Res. 17 (2000) 1374–1382.
[2] H.R. Costantino, L. Firouzabadian, C. Wu, K.G. Carrasquillo, K. Griebenow, S.E. Zale, M.A. Tracy, Protein spray freeze drying. 2. Effect of formulation variables on particle size and stability, J. Pharm. Sci. 91 (2002) 388–395.
[3] Y.-F. Maa, P.-A. Nguyen, T. Sweeney, S.J. Shire, C.C. Hsu, Protein inhalation powders: spray drying vs spray freeze drying, Pharm. Res. 16 (1999) 249–254.
[4] Y.-F. Maa, P.-A. Nguyen, Method of spray freeze drying proteins for pharmaceutical administration, US Patent 6,282,282 (2002).
[5] H. Leuenberger, Spray freeze-drying – the process of choice for low water soluble drugs?, J Nanoparticle Res. 4 (2002) 111–119.
[6] C. Sonner, Y.-F. Maa, G. Lee, Spray-freeze-drying for protein powder preparation: particle characterization and a case study with trypsinogen stability, J. Pharm. Sci. 91 (2002) 2122–2139.
[7] Y.-F. Maa, C. Shu, M. Ameri, C.Y. Zuleger, J. Che, J.E. Osorio, L.G. Payne, D. Chen, Optimization of alum-adjuvanted vaccine powder formulation for epidermal powder immunization, Pharm. Res. 20 (2002) 969–977.
[8] Y.-F. Maa, M. Ameri, C. Shu, L.G. Payne, D. Chen, Influenza vaccine powder formulation development: spray-freeze-drying and stability evaluation, J. Pharm. Sci. 93 (2004) 1912–1923.
[9] J. Hu, T.L. Rodgers, J.N. Brown, T.J. Young, K.P. Johnson, R.O. Williams, Improvement of dissolution rates of poorly water soluble APIs using novel spray freeze into liquid technology, Pharm. Res. 19 (2002) 1278–1284.
[10] H. Sadikoglu, A.I. Liapis, Mathematical modeling of the primary and secondary drying stages of bulk freeze drying in trays: parameter estimation and model discrimination by comparison of theoretical results with experimental data, Drying Technol. 15 (1997) 791–810.
[11] P. Sheehan, A.I. Liapis, Modeling of the primary and secondary drying stages of the freeze drying of pharmaceutical products in vials: numerical results obtained from the solution of a dynamic and spatially multi-dimensional lyophilization model for different operational policies, Biotechnol. Bioeng. 60 (1998) 712–728.
[12] K.H. Gan, R. Bruttini, O.K. Crosser, A.I. Liapis, Freeze-drying of pharmaceuticals in vials on trays: effects of drying chamber wall temperature and tray side on lyophilization performance, Int. J. Heat Mass Transf. 48 (2005) 1675–1687.
[13] C.S. Song, J.H. Nam, C.-J. Kim, S.T. Ro, A finite volume analysis of vacuum freeze drying processes of skim milk solution in trays and vials, Drying Technol. 20 (2002) 283–305.

[14] A.I. Liapis, R. Bruttini, Freeze drying, in: A.S. Mujumdar (Ed.), Handbook of Industrial Drying, third ed., Taylor & Francis, Boca Raton, Florida, USA, 2006, pp. 257–283.
[15] R. Bruttini, O.K. Crosser, A.I. Liapis, Exergy analysis of the freezing stage of the freeze drying process, Drying Technol. 19 (2001) 2303–2313.
[16] L. Chang, D. Shepherd, J. Sun, X. Tang, M.J. Pikal, Effect of sorbitol and residual moisture on the stability of lyophilized antibodies: implications for the mechanism of protein stabilization in the solid state, J. Pharm. Sci. 94 (2005) 1445–1455.
[17] G.N. Panagopoulos, R. Bruttini, A.I. Liapis, A molecular dynamics modeling and simulation study on determining the molecular mechanism by which formulations based on trehalose could stabilize biomolecules during freeze drying, in: I. Farkas (Ed.), Proceedings of the 15th International Drying Symposium (IDS 2006, August 20–23, 2006, Budapest, Hungary), vol. A, 2006, pp. 114–119.
[18] A.I. Liapis, R. Bruttini, Exergy analysis of freeze drying of pharmaceuticals in vials on trays, Int. J. Heat Mass Transf. 51 (2008) 3854–3868.
[19] M.J. Pikal, Freeze drying, Encyclopedia of Pharmaceutical Technology, vol. 6, Marcel Dekker, New York, NY, USA, 1992, pp. 275–303.
[20] C.D. Holland, A.I. Liapis, Computer Methods for Solving Dynamic Separation Problems, McGraw-Hill Book Company, New York, NY, USA, 1983.
[21] R.B. Bird, W.E. Stewart, E.N. Lightfoot, Transport Phenomena, second ed., Wiley & Sons, New York, NY, USA, 2002.
[22] A.V. Luikov, Systems of differential equations of heat and mass transfer in capillary-porous bodies, Int. J. Heat Mass Transf. 18 (1975) 1–14.
[23] Y.C. Fey, M.A. Boles, An analytical study of the effect of convection heat transfer on the sublimation of a frozen semi-infinite porous medium, Int. J. Heat Mass Transf. 30 (1987) 771–779.
[24] Y.C. Fey, M.A. Boles, An analytical study of the effect of the Darcy and Ficks laws on the sublimation of a frozen porous medium, ASME J. Heat Transf. 109 (1987) 1045–1048.
[25] Z.H. Wang, M.H. Shi, The effects of sublimation–condensation region on heat and mass transfer during microwave freeze drying, ASME J. Heat Transf. 120 (1998) 654–660.
[26] Z.H. Wang, M.H. Shi, Numerical study on sublimation–condensation phenomena during microwave freeze drying, Chem. Eng. Sci. 53 (1998) 3189–3197.
[27] J.H. Petropoulos, J.K. Petrou, A.I. Liapis, Network model investigation of gas transport in bidisperse porous adsorbents, Ind. Eng. Chem. Res. 30 (1991) 1281–1289.
[28] J.J. Meyers, A.I. Liapis, Network modeling of the convective flow and diffusion of molecules adsorbing in monoliths and in porous particles packed in a chromatographic column, J. Chromatogr. A 852 (1999) 3–23.
[29] A.I. Liapis, B.A. Grimes, The effect of the pore structure and zeta potential of porous polymer monoliths on separation performance in ion exchange mode, J. Sep. Sci. 30 (2007) 648–657.
[30] A.I. Liapis, R.J. Litchfield, Optimal control of a freeze dryer I: theoretical development and quasi steady state analysis, Chem. Eng. Sci. 34 (1979) 975–981.
[31] R.J. Litchfield, A.I. Liapis, Optimal control of a freeze dryer II: dynamic analysis, Chem. Eng. Sci. 37 (1982) 45–55.
[32] R.J. Litchfield, F.A. Farhadpour, A.I. Liapis, Cyclical pressure freeze drying, Chem. Eng. Sci. 36 (1981) 1233–1238.
[33] H. Sadikoglu, A.I. Liapis, O.K. Crosser, Optimal control of the primary and secondary drying stages of bulk solution freeze drying in trays, Drying Technol. 16 (1998) 399–431.
[34] H. Sadikoglu, M. Ozdemir, M. Seker, Optimal control of the primary drying stage of freeze drying of solutions in vials using variational calculus, Drying Technol. 21 (2003) 1307–1331.
[35] P. Sheehan, H. Sadikoglu, A.I. Liapis, Dynamic behavior and process control of the primary and secondary drying stages of freeze drying of pharmaceuticals in vials, in: C.B. Akritidis, D. Marinos-Kouris, G.D. Saravakos (Eds.), Proceedings of the 11th International Drying Symposium (IDS 1998, August 19–22, 1998, Halkidiki, Greece), vol. C, 1998, pp. 1727–1740.
[36] A.I. Liapis, H. Sadikoglu, Dynamic pressure rise in the drying chamber as a remote sensing method for monitoring the temperature of the product during the primary drying stage of freeze drying, Drying Technol. 16 (1998) 1153–1171.
[37] S. Whitaker, Simultaneous Heat, Mass, and Momentum Transfer in Porous Media: A Theory of Drying, Advances in Heat Transfer, vol. 13, Academic Press, New York, NY, USA, 1977, pp. 119–203.
[38] M.J. Millman, A.I. Liapis, J.M. Marchello, An Analysis of the lyophilization process using a sorption–sublimation model and various operational policies, AIChE J. 31 (1985) 1594–1604.
[39] P.J. Gloor, O.K. Crosser, A.I. Liapis, Dusty-gas parameters of activated carbon adsorbent particles, Chem. Eng. Commun. 59 (1987) 95–105.
[40] R. Jackson, Transport in Porous Catalysts, Elsevier, Amsterdam, The Netherlands, 1977.
[41] E.A. Mason, A.P. Malinauskas, Gas Transport in Porous Media: The Dusty-Gas Model, Elsevier, New York, NY, USA, 1983.
[42] V. Levi, Q. Ruan, E. Gratton, 3-D particle tracking in a two-photon microscope: application to the study of molecular dynamics in cells, Biophys. J. 88 (2005) 2919–2928.
[43] X. Zhang, J.-C. Wang, K.M. Lacki, A.I. Liapis, Construction by molecular dynamics modeling and simulations of the porous structures formed by dextran polymer chains attached on the surface of the pores of a base matrix: characterization of porous media, J. Phys. Chem. B 109 (2005) 21028–21039.
[44] T. Ragan, H. Huang, P. So, E. Gratton, 3D particle tracking on a two-photon microscope, J. Fluoresc. 16 (2006) 325–336.
[45] M. Kaviany, Principles of Heat Transfer in Porous Media, second ed., Springer, New York, NY, USA, 1999.
[46] J. Marti, K. Mauersberger, A survey and new measurements of ice vapor pressure at temperatures between 170 and 250 K, Geophys. Res. Lett. 20 (1993) 363–366.
[47] K.H. Gan, R. Bruttini, O.K. Crosser, A.I. Liapis, Heating policies during the primary and secondary drying stages of the lyophilization process in vials: effects of the arrangement of vials in clusters of square and hexagonal arrays on trays, Drying Technol. 22 (2004) 731–769.
[48] C.N. Satterfield, Mass Transfer in Heterogeneous Catalysis, M.I.T. Press, Cambridge, MA, USA, 1970.
[49] G.F. Froment, K.B. Bischoff, Chemical Reactor Analysis and Design, John Wiley & Sons, New York, NY, USA, 1979.
[50] C.J. Geankoplis, Transport Processes and Unit Operations, third ed., Prentice Hall, Englewood Cliffs, New Jersey, USA, 1993.